JACS
JOURNAL OF THE AMERICAN CHEMICAL SOCIETY
Communication
pubs.acs.org/JACS

# Atomic Linkage Flexibility Tuned Isotropic Negative, Zero, and Positive Thermal Expansion in $MZrF_6$ (M = Ca, Mn, Fe, Co, Ni, and Zn)

Lei Hu,[†] Jun Chen,*[,†] Jiale Xu,[†] Na Wang,[†] Fei Han,[†] Yang Ren,[‡] Zhao Pan,[†] Yangchun Rong,[†] Rongjin Huang,[§] Jinxia Deng,[†] Laifeng Li,[§] and Xianran Xing[†]

[†]Department of Physical Chemistry, University of Science and Technology Beijing, Beijing 100083, China
[‡]X-ray Science Division, Argonne National Laboratory, Argonne, Illinois 60439, United States
[§]Key Laboratory of Cryogenics, Technical Institute of Physics and Chemistry, Chinese Academy of Sciences, Beijing 100190, China

Supporting Information

**ABSTRACT:** The controllable isotropic thermal expansion with a broad coefficient of thermal expansion (CTE) window is intriguing but remains challenge. Herein we report a cubic $MZrF_6$ series (M = Ca, Mn, Fe, Co, Ni and Zn), which exhibit controllable thermal expansion over a wide temperature range and with a broader CTE window ($-6.69$ to $+18.23 \times 10^{-6}$/K). In particular, an isotropic zero thermal expansion (ZTE) is achieved in $ZnZrF_6$, which is one of the rarely documented high-temperature isotropic ZTE compounds. By utilizing temperature-dependent high-energy synchrotron X-ray total scattering diffraction, it is found that the flexibility of metal···F atomic linkages in $MZrF_6$ plays a critical role in distinct thermal expansions. The flexible metal···F atomic linkages induce negative thermal expansion (NTE) for $CaZrF_6$, whereas the stiff ones bring positive thermal expansion (PTE) for $NiZrF_6$. Thermal expansion could be transformed from striking negative, to zero, and finally to considerable positive though tuning the flexibility of metal···F atomic linkages by substitution with a series of cations on M sites of $MZrF_6$. The present study not only extends the scope of NTE families and rare high-temperature isotropic ZTE compounds but also proposes a new method to design systematically controllable isotropic thermal expansion frameworks from the perspective of atomic linkage flexibility.

Negative thermal expansion (NTE) is an intriguing thermophysical property, which distributes in diverse solids.[1−3] One of mainstream NTE materials share open framework structures, involving the cooperative rotation of metal coordination polyhedra, like $ZrW_2O_8$,[1] $Zr_{1-x}Sn_xMo_2O_8$,[4] $Sc_{1-x}M_xF_3$,[5,6] and topologically flexible frameworks.[7] Besides, other NTEs originate from valence fluctuation in $BiNiO_3$,[8] magnetic ordering variation,[9,10] and spontaneous volume ferroelectrostriction in $PbTiO_3$ ferroelectrics.[3,11]

Actually, cubic NTE isostructures with a controllable coefficient of thermal expansion (CTE) are rare[4,7,10] but fairly desirable for both fundamental research and technological applications. It is valuable that NTE could be chemically modified to positive thermal expansion (PTE), especially achieving scarce but critical isotropic zero thermal expansion (ZTE). Most NTE lattices exhibit highly flexible framework characteristic. Their controllable CTEs have been well designed within the negative region, like $LnCo(CN)$,[7b] $MPt(CN)_6$,[12] $M_3[Co(CN)_6]\cdot nH_2O$,[13] and $M_2O$.[14] However, it is scarce to find that the CTE window could be transformed to ZTE or even PTE. Until now, systematic design of an isotropic NTE framework to achieve an extended CTE window has only been reported in rarities, such as $Zr_{1-x}Sn_xMo_2O_8$,[4] $(Sc_{1-x}M_x)F_3$,[6a,15] and some antiperovskite nitrides.[10] Furthermore, low frequency phonon modes corresponding to NTE is easily overwhelmed by high frequency ones. With increasing temperature, the latter becomes dominant, overcomes the NTE contribution and produces considerable PTE. It is not difficult to understand that the majority of isotropic ZTEs could not persist up to high temperature.[16b] Accordingly, it is a great challenge to find a framework with appropriate flexibility to design systematically a series of controllable CTEs, especially to achieve isotropic high-temperature ZTE.

Herein we report a systematically controllable thermal expansion (NTE, ZTE, and PTE) with a much broader CTEs ($-6.69$ to $+18.23 \times 10^{-6}$/K) over a wide temperature range (300 to 673 K) in $MZrF_6$ series (M = Ca, Mn, Fe, Co, Ni, and Zn). In particular, rarely documented isotropic ZTE has been achieved in $ZnZrF_6$. The controllable thermal expansion is correlated closely with the flexibility of the metal···F atomic linkages. The present study extends the scope of controllable NTE compounds not only possessing a broader CTE window but also functionalizing over a wide high-temperature range. The proposed method of atomic linkage flexibility tuned NTE could provide a good example to design controllable NTE framework solids.

A series of $MZrF_6$ isostrucutres (M = Ca, Mn, Fe, Co, Ni, and Zn) were prepared by a solid-state reaction method (see Supporting Information). At ambient condition, all compounds adopt double $ReO_3$-type structure and crystallize with $Fm\bar{3}m$ cubic lattice. In detail, $MZrF_6$ comprises the combination of $MF_6$ octahedra alternating with $ZrF_6$ ones. Taking $CaZrF_6$ for instance, Ca (yellow sphere), Zr (cyan), and F (red) atoms occupy Wyckoff sites 2a (0, 0, 0), 2b (0.5, 0.5, 0.5), and 24e ($x$, 0, 0), respectively (Figure 1).

**Received:** August 21, 2016
**Published:** October 26, 2016





DOI: 10.1021/jacs.6b08746
J. Am. Chem. Soc. 2016, 138, 14530−14533

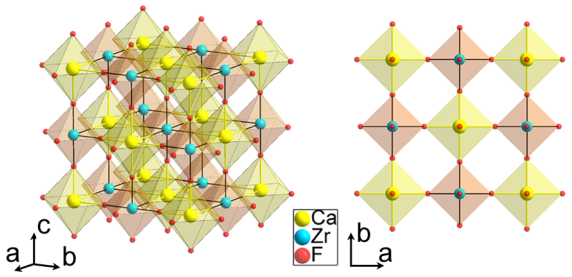


**Figure 1.** Crystal structure of $MZrF_6$ (M denotes Ca here as an example) with $MF_6$ (yellow) and $ZrF_6$ octahedra (red).

Variable temperature XRD of $MZrF_6$ has been analyzed to investigate thermal expansion. It is interesting to find that although $MZrF_6$ series share the same cubic symmetry, the magnitude of NTE varies systematically with substitution across the *3d*-row (Figure 2a). The lattice constant of $CaZrF_6$

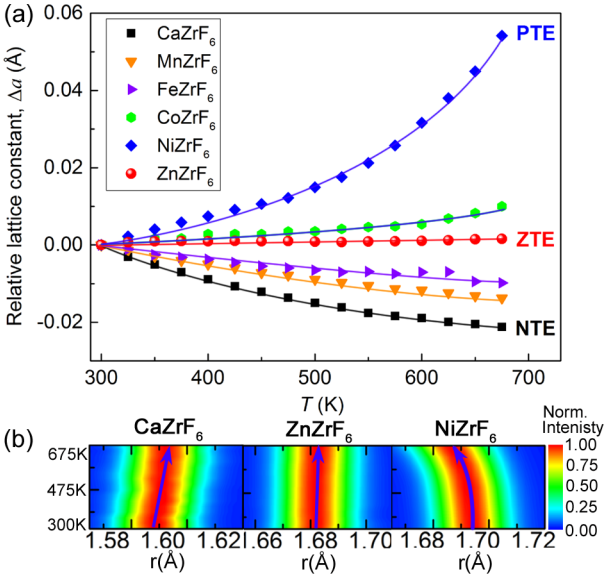


**Figure 2.** (a) Temperature dependence of lattice constant change relative to the RT value for $MZrF_6$ (M = Ca, Mn, Fe, Co, Ni, and Zn). (b) Contour plots of the normalized intensity for the (200) peaks of SXRD patterns, respectively.

decreases smoothly with increasing temperature, exhibiting a strong NTE with a linear CTE ($\alpha_l = -6.69 \times 10^{-6}$/K, RT to 675 K, Figure 2a). It is in good agreement with the previous report.[17a] This CTE is well approaching that of $ZrW_2O_8$ ($\alpha_l = -9.1 \times 10^{-6}$/K)[1] and approximately twice that of $ScF_3$ ($\alpha_l = -3.1 \times 10^{-6}$/K, 300−900 K).[6a] However, with the replacement of Mn or Fe for Ca, the NTE is continuously dampened ($\alpha_l = -4.47 \times 10^{-6}$/K for $MnZrF_6$, and $-3.24 \times 10^{-6}$/K for $FeZrF_6$). Intriguingly, the isotropic ZTE in the composition of $ZnZrF_6$ is highlighted by the miniscule fluctuation of lattice constant as shown in Figure 2a. Its $\alpha_l$ is $+0.52 \times 10^{-6}$/K, which covers a broad temperature range (RT to 675 K). Slight and considerable PTE occurs in $CoZrF_6$ ($\alpha_l = +3.33 \times 10^{-6}$/K) and $NiZrF_6$ ($\alpha_l = +18.23 \times 10^{-6}$/K), respectively. As represented in Figure 2b, contour plots of the (200) peaks of $MZrF_6$ (M = Ca, Zn, and Ni) shift to higher, barely shift, and move to lower angle regions, respectively. This directly depicts their strong NTE, ZTE, and considerable PTE properties. Additionally, low temperature thermal expansions of these compounds are presented in Figure S2 and Table S1. In detail, lattice constants, CTEs, and ionic radii of $MZrF_6$ series are listed in Table S2. A correlation between CTE and ionic radius is found and depicted in Figure S3. Theoretical calculations were performed to investigate the bonding feature in two representative compounds of $CaZrF_6$ and $NiZrF_6$ (Table S3 and Figure S4).

The application of NTE materials necessitates a broader CTE window. However, until now, few of isotropic NTE compounds with open-frameworks could obtain a wide CTE window by chemical substitutions. The controllable CTEs of most NTE compounds are restricted in the negative region. Very few compounds have been found to reveal controllable CTEs covering from negative to positive. For example, $Zr_{1-x}Sn_xMo_2O_8$ solids show a controllable CTE window ($\alpha_l = -5.7 - +7.9 \times 10^{-6}$/K),[4] and that of $ScF_3$-based fluorides ($\alpha_l = -3.3 - +3.3 \times 10^{-6}$/K).[6a] The representative isotropic NTE series are summarized in Table S4. In comparison, a surprisingly broader CTE window ($\alpha_l = -6.69 - +18.23 \times 10^{-6}$/K) has been achieved in this $MZrF_6$ series. The controllable isotropic thermal expansion covers a wider CTE window from strong NTE to considerable PTE. It is important to note that the controllable CTEs of $MZrF_6$ cover that of most compounds. On the one hand, its strong NTE is comparable with typical isotropic NTEs, like $ZrW_2O_8$ ($-9.1 \times 10^{-6}$/K)[1] or $ZrMo_2O_8$ ($-5.9 \times 10^{-6}$/K).[4] On the other hand, its PTE ($+18.23 \times 10^{-6}$/K) is as considerable as the strong expansion ceramics or metals, such as $Al_2O_3$ ($+7.8 \times 10^{-6}$/K),[2] Fe ($+12 \times 10^{-6}$/K),[10a] and Cu ($+16.64 \times 10^{-6}$/K).[2] Besides, the controllable thermal expansion could also be achieved by forming solid solutions between NTE and PTE $MZrF_6$, such as $(Mn_{1-x}Ni_x)ZrF_6$ and $(Fe_{1-x}Ni_x)ZrF_6$. For example, a ZTE property has been found in $(Fe_{0.5}Ni_{0.5})ZrF_6$ ($\alpha_l = +0.17 \times 10^{-6}$/K).

Furthermore, it remains a challenge to achieve an isotropic ZTE over a broad temperature range. Until now, remarkable isotropic ZTE has been found in limited compounds, such as $Zr_{0.4}Sn_{0.6}Mo_2O_8$ (up to 600 K),[4] $Zn_4B_6O_{13}$ (13−110 K),[18] $N(CH_3)_4CuZn(CN)_4$ (200−400 K),[19] $Fe[Co(CN)_6]$ (4.2−300 K),[20] $Mn_{3.243}Ni_{0.747}N$ (140−230 K),[16a] $Mn_3(Cu_{0.5}Sn_{0.5})N$ (307−355 K),[10b] $TaO_2F$ (RT to 800 K),[21] and $(Sc_{1-x}M_x)F_3$ (RT to 900 K).[5b,6a] Interestingly, given the systematically controllable CTEs in $MZrF_6$ series, a satisfactorily isotropic ZTE has been achieved in $ZnZrF_6$ ($\alpha_l = +0.52 \times 10^{-6}$/K) which spans a wide temperature range (RT to 675 K). This isotropic ZTE of $ZnZrF_6$ could enrich the diversity of high temperature isotropic ZTE candidates.

Why does the thermal expansion of $MZrF_6$ behave remarkably differently, even though they have the identical cubic crystallographic symmetry? It is presumably that the local vibrational dynamics plays a critical role in their thermal expansion. To elucidate the underlying vibrational mechanism, temperature-dependent synchrotron X-ray pair distribution function (XPDF) was employed. Before the discussion on XPDF, two distinct rocking models are introduced here. As shown in Figure 3a, one is the flexible rocking model (FRM) and the other is the weak rocking model (WRM). The substructure consists of vertex-linked octahedra of $MF_6$ (yellow) and $ZrF_6$ (pink). The black arrows 1 and 2 indicate the distances of the M···F atomic linkages in which F atom is next nearest neighbor to M. Firstly, the distances of 1 and 2 are identical if no rocking occurs. However, on heating the coupled rotation of octahedra induces a distribution of distances of the


DOI: 10.1021/jacs.6b08746
J. Am. Chem. Soc. 2016, 138, 14530−14533

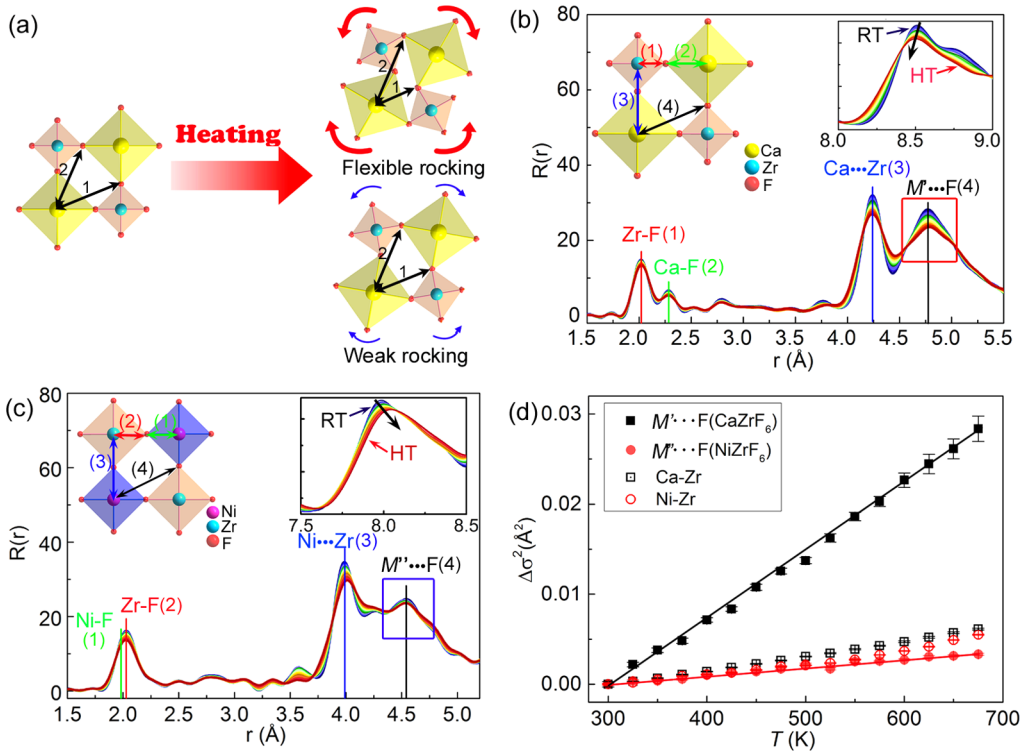


**Figure 3.** (a) Two rocking models of $MZrF_6$ substructures. Temperature dependence of XPDF radial distribution function, $R(r)$, from RT to HT, for (b) $CaZrF_6$, and (c) $NiZrF_6$. The upper-left insets in panels b and c show distinct peaks corresponding to atomic pairs marked by the same color arrows in the two substructures. The upper-right insets show the metal···metal peaks in $CaZrF_6$ or $NiZrF_6$. (d) Relative $\sigma^2(T)$ for different peaks of $CaZrF_6$ and $NiZrF_6$.

M···F linkages. In the FRM, flexible rotation yields a wide distribution of distances of the M···F linkages, whereas in the WRM a slight variation occurs. As a result, the NTE may be produced in the FRM not in the WRM.

As shown in Figure 3b,c, the atomic linkages can be identified. For example, the atomic pairs of Ca−F, Zr−F, Ca···Zr, and M′···F (M′ = Ca or Zr) for NTE $CaZrF_6$ are approximately at 2.05, 2.28, 4.25, and 4.75 Å, respectively (Figure 3b). For PTE $NiZrF_6$, Ni···Zr and M′···F (M′ = Ni or Zr) peaks are at 4.0 and 4.51 Å. It needs to note that the Ni−F and Zr−F peaks merge into a broad one due to the similar ionic sizes of $Ni^{2+}$ and $Zr^{4+}$ ($Ni^{2+}$ = 0.69 Å, and $Zr^{4+}$ = 0.72 Å).[22] This gives rise to the difficulty to distinguish the similar lengths of Ni−F and Zr−F bonds by the present XPDF, even with an adequate resolution ($Q$ = 26 $Å^{-1}$). The upper-right inset of Figure 3b mainly shows the contraction of Ca···Ca or Zr···Zr correlations on heating. This contraction is greatly consistent with its macroscopic NTE behavior of $CaZrF_6$. Contrarily, the distance of Ni···Ni or Zr···Zr correlations (Figure 3c, the upper-right inset) enhances greatly on heating, also confirming its lattice PTE.

Most importantly, the M′···F linkage of NTE $CaZrF_6$ at 4.8 Å denoted as (4) (marked by the red box) in Figure 3b exhibits strong temperature sensitiveness. The M′···F peak broadens greatly. Simultaneously, it drops in height from RT to 675 K, approximately to ∼84% of the primary peak height (Figure 3b). In sharp contrast, the M″···F correlation of PTE $NiZrF_6$ (marked by the blue box) seems to be frozen and barely changes in height (only decreases to 96% up to 675 K). Quantitively, the stiffness of atomic linkages could be revealed by the variation of $\sigma^2$ as a function of temperature. Theoretically, $\sigma^2/T$ correlates positively with $k_B\omega^{-2}$ ($\sigma$, the Gaussian FWHM; $k_B$, Boltzmann constant; $\omega$, effective vibrational frequency). The larger $\sigma^2/T$ value indicates the lower $\omega^2$, the smaller force constant, and the higher flexibility of atomic linkage. The relative $\sigma^2$ ($T$) plots are depicted in Figure 3d. Intriguingly, only the $\sigma^2$ of M′···F for NTE $CaZrF_6$ increases rapidly with increasing temperature. Its slope is 7.56 × $10^{-5}$ $Å^2$/K (Figure 3d), which is similar to that of Zr−W linkages (2.2 × $10^{-5}$ $Å^2$/K) in $ZrW_2O_8$.[1b] The similarity in the slope may explain the similar magnitude of NTE for $CaZrF_6$ and $ZrW_2O_8$. However, the $\sigma^2$ of M″···F of PTE $NiZrF_6$ increases with such a slow rate. Its slope (0.89 × $10^{-5}$ $Å^2$/K) is almost 1 order smaller than that of NTE $CaZrF_6$. The larger slope suggests the flexible M′···F linkage and the wider distribution of M′···F distances in NTE $CaZrF_6$, whereas the smaller one indicates the stiff M″···F linkage and its narrow distance distribution in PTE $NiZrF_6$. This could be also supported by our theoretical calculation, in which the charge cloud in NTE $CaZrF_6$ is more localized whereas more covalent in PTE $NiZrF_6$. This demonstrates the Ca−F bond is weaker than the Ni−F one (Figure S4). As with the previous discussion for Figure 3a, the most significant deviation for lattice dynamics lies in the M···F linkages of $CaZrF_6$ and $NiZrF_6$. The soft M′···F linkages of $CaZrF_6$ allows a flexible or intense coupled rocking of $CaF_6$ and $ZrF_6$ octahedra, which has been indicated by the lower-frequency $F_{2g}$ phonon mode.[17b] However, the restricted M″···F linkage of PTE $NiZrF_6$ only permits a weak rocking. The physical picture is visualized in the Figure 3a by the two different rocking models of FRM and WRM. In NTE $CaZrF_6$, the flexible rocking of polyhedra is strong enough to counterbalance the PTE contribution originating from chemical bonds, giving rise to the shrinkage of Ca···Ca and Zr···Zr linkages and thus to NTE. However, with chemical substitution


DOI: 10.1021/jacs.6b08746
J. Am. Chem. Soc. 2016, 138, 14530−14533

with M-site atoms, the M···F linkages of $MZrF_6$ progressively become stiffer and the local transverse vibrations turn to be dampened in magnitude. Ultimately, thermal expansion of $MZrF_6$ transforms from negative in $CaZrF_6$ to the considerable positive in $NiZrF_6$. Meanwhile, the temperature dependence of rocking angle demonstrates an intense thermal vibration of fluorine atoms in NTE $CaZrF_6$ whereas a fairly weak one in PTE $NiZrF_6$ (Figure S6).

For NTE flexible geometries, the present study provides a possibility to design systematically materials with desirable thermal expansion by finely tuning the flexibility of correlated atomic linkages. The atomic linkage flexibility tuned thermal expansion could be referred to elucidate the local vibrational mechanism of most NTE framework compounds.

In summary, systematical design of controllable isotropic thermal expansions including NTE, ZTE, and PTE have been observed in $MZrF_6$ analogues (M = Ca, Mn, Fe, Co, Ni, and Zn). The tunable thermal expansion exhibits an extended CTE window ($-6.69$ to $+18.23 \times 10^{-6}$/K). Intriguingly, the isotropic ZTE property has also been achieved in $ZnZrF_6$ over a wide temperature range. Temperature dependence of XPDF analysis provides a deep insight into the lattice dynamics of $MZrF_6$. The flexibility of the M···F linkages, involving the rocking model, plays a critical role in thermal expansion behavior. The flexible M···F linkages enhance the octahedral rocking and thus produce NTE for $CaZrF_6$, whereas stiffer ones weaken the rocking which dampens thermal expansion from negative, to zero, and finally to positive by simply substituting *3d*-row cations for Ca. The atomic linkage flexibility tuned isotropic thermal expansion provides a new method to design controllable thermal expansion materials and could be utilized in extensive framework structures.

## ■ ASSOCIATED CONTENT

### Supporting Information

The Supporting Information is available free of charge on the ACS Publications website at DOI: 10.1021/jacs.6b08746.

Sample preparation, experimental methods, data analysis procedures and first-principle calculations (PDF)

## ■ AUTHOR INFORMATION


### Corresponding Author

*junchen@ustb.edu.cn


### Notes

The authors declare no competing financial interest.

## ■ ACKNOWLEDGMENTS

This work was supported by the National Natural Science Foundation of China (grant nos. 21322102, 91422301, 21231001, and 21590793), the Changjiang Young Scholars Award. National Program for Support of Top-Notch Young Professionals, the Fundamental Research Funds for the Central Universities, China (FRF-TP-14-012C1). This research used resources of the Advanced Photon Source, a U.S. Department of Energy (DOE) Office of Science User Facility operated for the DOE Office of Science by Argonne National Laboratory under Contract No. DE-AC02-06CH11357. We acknowledge the discussions on PDF analysis with Dr. R.Z. Yu and Dr. E. Bozin, and theoretical calculation with Dr. X.X. Jiang and Prof. Z.S. Lin.

## ■ REFERENCES


(1) (a) Mary, T. A.; Evans, J. S. O.; Vogt, T.; Sleight, A. W. *Science* **1996**, *272*, 90. (b) Tucker, M. G.; Goodwin, A. L.; Dove, M. T.; Keen, D. A.; Wells, S. A.; Evans, J. S. *Phys. Rev. Lett.* **2005**, *95*, 255501.

(2) Evans, J. S. *J. Chem. Soc., Dalton Trans.* **1999**, *19*, 3317.

(3) Chen, J.; Hu, L.; Deng, J. X.; Xing, X. R. *Chem. Soc. Rev.* **2015**, *44*, 3522. (b) Takenaka, K. *Sci. Technol. Adv. Mater.* **2012**, *13*, 013001.

(4) Tallentire, S. E.; Child, F.; Fall, I.; Vellazarb, L.; Evans, I. R.; Tucker, M. G.; Keen, D. A.; Wilson, C.; Evans, J. S. *J. Am. Chem. Soc.* **2013**, *135*, 12849.

(5) (a) Greve, B. K.; Martin, K. L.; Lee, P. L.; Chupas, P. J.; Chapman, K. W.; Wilkinson, A. P. *J. Am. Chem. Soc.* **2010**, *132*, 15496. (b) Morelock, C.; Gallington, L.; Wilkinson, A. *Chem. Mater.* **2014**, *26*, 1936.

(6) (a) Hu, L.; Chen, J.; Fan, L.; Ren, Y.; Rong, Y.; Pan, Z.; Deng, J.; Yu, R.; Xing, X. *J. Am. Chem. Soc.* **2014**, *136*, 13566. (b) Hu, L.; Chen, J.; Sanson, A.; Wu, H.; Rodriguez, C.; Olivi, L.; Ren, Y.; Fan, L.; Deng, J. X.; Xing, X. R. *J. Am. Chem. Soc.* **2016**, *138*, 8320.

(7) (a) Hibble, S. J.; Chippindale, A. M.; Marelli, E.; Kroeker, S.; Michaelis, V. K.; Greer, B. J.; Aguiar, P. M.; Bilbe, E. J.; Barney, E. R.; Hannon, A. C. *J. Am. Chem. Soc.* **2013**, *135*, 16478. (b) Duyker, S. G.; Peterson, V. K.; Kearley, G. J.; Ramirez-Cuesta, A. J.; Kepert, C. J. *Angew. Chem., Int. Ed.* **2013**, *52*, 5266.

(8) Azuma, M.; Chen, W. T.; Seki, H.; Czapski, M.; Oka, K.; Mizumaki, M.; Attfield, J. P. *Nat. Commun.* **2011**, *2*, 347.

(9) (a) Mohn, P. *Nature* **1999**, *400*, 18. (b) Huang, R. J.; Liu, Y.; Fan, W.; Tan, J.; Xiao, F.; Qian, L.; Li, L. F. *J. Am. Chem. Soc.* **2013**, *135*, 11469.

(10) (a) Takenaka, K.; Takagi, H. *Appl. Phys. Lett.* **2005**, *87*, 261902. (b) Takenaka, K.; Takagi, H. *Appl. Phys. Lett.* **2009**, *94*, 131904.

(11) (a) Chen, J.; Wang, F.; Huang, Q.; Hu, L.; Song, X.; Deng, J.; Yu, R.; Xing, X. *Sci. Rep.* **2013**, *3*, 3. (b) Chen, J.; Fan, L. L.; Ren, Y.; Pan, Z.; Deng, J. X.; Yu, R. B.; Xing, X. R. *Phys. Rev. Lett.* **2013**, *110*, 115901.

(12) Chapman, K. W.; Chupas, P. J.; Kepert, C. J. *J. Am. Chem. Soc.* **2006**, *128*, 7009.

(13) Adak, S.; Daemen, L. L.; Hartl, M.; Williams, D.; Summerhill, J.; Nakotte, H. *J. Solid State Chem.* **2011**, *184*, 2854.

(14) Tiano, W.; Dapiaggi, M.; Artioli, G. *J. Appl. Crystallogr.* **2003**, *36*, 1461.

(15) Hu, L.; Chen, J.; Fan, L. L.; Ren, Y.; Huang, Q. Z.; Sanson, A.; Jiang, Z.; Zhou, M.; Rong, Y. C.; Wang, Y.; Deng, J. X.; Xing, X. R. *Adv. Mater.* **2015**, *27*, 4592.

(16) (a) Deng, S.; Sun, Y.; Wu, H.; Huang, Q.; Yan, J.; Shi, K.; Malik, M.; Lu, H.; Wang, L.; Huang, R.; Li, L.; Wang, C. *Chem. Mater.* **2015**, *27*, 2495. (b) Song, X. Y.; Sun, Z. H.; Huang, Q. Z.; Rettenmayr, M.; Liu, X.; Seyring, M.; Li, G.; Rao, G.; Yin, F. *Adv. Mater.* **2011**, *23*, 4690.

(17) (a) Hancock, J. C.; Chapman, K. W.; Halder, G. J.; Morelock, C. R.; Kaplan, B. S.; Gallington, L. C.; Bongiorno, A.; Han, C.; Zhou, S.; Wilkinson, A. P. *Chem. Mater.* **2015**, *27*, 3912. (b) Sanson, A.; Giarola, M.; Mariotto, G.; Hu, L.; Chen, J.; Xing, X. R. *Mater. Chem. Phys.* **2016**, *180*, 213.

(18) Jiang, X. X.; Molokeev, M. S.; Gong, P. F.; Yang, Y.; Wang, W.; Wang, S. H.; Wu, S. F.; Wang, Y. X.; Huang, R. J.; Li, L. F.; Wu, Y. C.; Xing, X. R.; Lin, Z. S. *Adv. Mater.* **2016**, *28*, 7936.

(19) Phillips, A. E.; Halder, G. J.; Chapman, K. W.; Goodwin, A. L.; Kepert, C. J. *J. Am. Chem. Soc.* **2010**, *132*, 10.

(20) Margadonna, S.; Prassides, K.; Fitch, A. N. *J. Am. Chem. Soc.* **2004**, *126*, 15390.

(21) Tao, J.; Sleight, A. *J. Solid State Chem.* **2003**, *173*, 45.

(22) Shannon, R. T. *Acta Crystallogr., Sect. A: Cryst. Phys., Diffr., Theor. Gen. Crystallogr.* **1976**, *32*, 751.




DOI: 10.1021/jacs.6b08746
J. Am. Chem. Soc. 2016, 138, 14530−14533